NASA TN D-59

TECHNICAL NOTE
D-59

INVESTIGATION OF VIBRATION CHARACTERISTICS OF CIRCULAR-ARC MONOCOQUE BEAMS

By Wilbur B. Fichter and Eldon E. Kordes

Langley Research Center
Langley Field, Va.

NATIONAL AERONAUTICS AND SPACE ADMINISTRATION

WASHINGTON

September 1959

NATIONAL AERONAUTICS AND SPACE ADMINISTRATION

TECHNICAL NOTE D-59

INVESTIGATION OF VIBRATION CHARACTERISTICS OF CIRCULAR-ARC MONOCOQUE BEAMS

By Wilbur B. Fichter and Eldon E. Kordes

SUMMARY

Experimental free-free vibration frequencies and nodal patterns of two 4-percent-thick monocoque beams, which differed only in cover-sheet thickness, are presented and comparisons are made between experimental and calculated beam frequencies. For the beam with thicker cover sheets, calculated frequencies were within 12 percent of the experimental frequencies for the first six bending modes and the first two torsion modes. For the other beam, comparable accuracies were obtained for only the first three bending modes.

INTRODUCTION

The solutions to aeroelastic problems associated with the trend toward the use of monocoque wings for high-speed aircraft call for information on the vibration characteristics of such structures.

Bending and torsional vibrations of hollow thin-walled cylindrical beams with a large number of rigid ribs have been investigated theoretically in several papers. (See, for example, refs. 1 and 2.) The accuracies of the frequencies calculated by these methods were shown in reference 3 to be quite satisfactory for box beams with rectangular cross sections and internal ribs; however, the suitabilities of the theories for application to monocoque and semimonocoque beams are not known, except for those with rectangular cross sections. (See ref. 4.)

In order to obtain experimental data on the vibration characteristics of monocoque beams representative of thick-skin wings, vibration tests were conducted on two 4-percent-thick beams with circular-arc cross sections. The purpose of the present paper is to present the experimental results for these beams and to show the agreement between experimental frequencies and frequencies calculated from beam theories.

EXPERIMENTAL INVESTIGATION

Description of Specimens

The dimensions of the two monocoque beams (beams 1 and 2) used in the present investigation are shown in figure 1. Each beam was made from two sheets of 7075-T6 aluminum alloy which were formed into circular-arc sections in the chordwise direction. The cross section was maintained by 1/2-inch-thick steel bulkheads located 10 inches from each end of the beam. With the weight of the steel bulkheads included, beam 1 weighed 215 pounds and beam 2 weighed 398 pounds.

Dimensions shown in figure 1 are nominal values, including that of the radius of curvature which was found to be a realistic average value. Both beams had a length of 140 inches, a chord of 40 inches, and a plan-form aspect ratio of 3.5. The maximum depth measured from the median lines of the cover sheets was 1.30 inches for beam 1 and 1.44 inches for beam 2. Each beam had a depth-chord ratio of approximately 0.04.

Test Equipment

The test equipment consisted of a shaker system and response measuring and recording instruments.

The shaker system consisted of four electromagnetic shakers, a control console, and a rotating-machine power supply with a frequency range from 5 to 500 cycles per second. Each shaker had a controlled force amplitude from 0 to 50 pounds and a phase control (0 or 180°) over the available frequency range. The total weight of the moving element of each shaker, including a velocity-sensitive signal generator, was 2.0 pounds. As many as 18 velocity pickups were attached to the beam and were connected through a switch panel to a cathode-ray oscilloscope. These pickups were used to monitor the motion of the vibrating beam. The weight of each pickup was 0.72 pound. The frequency of vibration was obtained from a Stroboconn frequency indicator. Detailed descriptions of this equipment are given in reference 3.

In addition to the measuring equipment described in reference 3, a portable probe pickup, which was not attached to the beam, was used to survey the motion of the beam at resonance. This pickup was similar in construction and weight to the velocity pickups except that a probe, which projected through the case, was attached to a signal generator coil moving in a magnetic field. The weight of the probe element was approximately 0.0022 pound and its spring constant was 9 pounds per inch. This pickup had a sensitivity of 94.5 millivolts per inch per second, an impedance of 850 ohms, and a frequency response that was essentially flat up to 500 cycles per second.

Test Setup and Instrumentation

An overall view of the test setup is shown in figure 2. The monocoque beam was suspended from wooden support frames by two flexible-steel aircraft cables attached to a small support fixture on each end of the beam. A small mass was attached to each of the support cables to facilitate detuning. The positions of the masses could be adjusted to change the natural frequency of the cables and hence eliminate troublesome resonances of the cables.

Two shakers were attached to each end of the beam as shown in figure 3. Also shown are the necked-down force connectors and one support cable and attachment. Figure 4 shows the locations of the shakers, velocity pickups, and counterweights used to keep the mass distribution symmetrical.

Test Procedure

In order to study the vibration characteristics of the two test beams, a shaker was attached to each corner of the beam (as shown in fig. 3) and the phase of each shaker was set to produce the desired motion. (For example, if symmetrical bending vibrations were being investigated, all four shakers were set to vibrate in phase with respect to the plane of the beam; if antisymmetrical torsion vibrations were being investigated, shakers on two diagonal corners were set to vibrate together and 180° out of phase with the other two shakers.)

In order to observe visually the motions of the beam, the output of one pickup was switched onto the Y-axis of the oscilloscope and the shaker force signal (current through the coil) was switched onto the X-axis. The power supply was then turned on and the force output of the shakers equalized. With the force controls set at a constant value, the frequency was slowly increased until the amplitude reached a maximum as determined from the pickup or signal generator output viewed on the oscilloscope. As an aid in obtaining the resonant frequency, the phase angle between the pickup signal and the force signal was observed from the Lissajous ellipse shown on the oscilloscope.

When a resonant frequency was reached, the frequency was held constant while probe pickups were used to locate all the null points, and hence the node lines. During this time the frequency was read on the Stroboconn frequency indicator and recorded along with its particular nodal pattern. After the resonance had been established and the data recorded, the frequency was increased until the next resonance was detected. In this manner all the resonant conditions in the frequency range from 15 to 170 cycles per second for beam 1 and from 15 to 245 cycles per second for beam 2 were investigated and recorded.

After all four parts of the vibration study were completed on each beam, the pickups and steel counterweights were removed and the tests were repeated to obtain the natural frequencies without the effect of these concentrated masses. For these tests, the signal generators were used to detect each resonance.

Experimental Results

In the frequency range covered by the tests on beam 1 with and without pickups and counterweights, the first 18 natural beam frequencies (10 bending and 8 torsion) were obtained and are presented in figure 5 with their corresponding nodal patterns.

For the tests on beam 2 with pickups and counterweights, the first 16 natural beam frequencies (8 bending and 8 torsion) were obtained, whereas 12 natural beam frequencies (6 bending and 6 torsion) were obtained with pickups and counterweights removed. These frequencies are presented in figure 6 with their corresponding nodal patterns.

Since the same general behavior noted for beam 1 was observed for beam 2 and since frequency differences caused by the addition of pickups and counterweights to either beam were 5 percent or less, beam 2 was not tested in the range above 150 cycles per second without pickups and counterweights.

In addition to the natural beam modes, several "extra" resonant conditions associated with panel vibration and chordwise deformation were detected and investigated. Their nodal patterns and corresponding frequencies are presented for beam 1 in figure 7 and for beam 2 in figure 8. In figures 7 and 8, plus or minus signs indicate the relative motion of each shaker.

THEORETICAL CALCULATIONS

The beam frequencies of the two monocoque beams were calculated by use of elementary theories for both bending and torsion, the theory of reference 1 for bending, and the theory of reference 2 for torsion. The theories of references 1 and 2 are based on the assumption of rigid cross section and neglect the effect of concentrated masses, panel vibrations, and cross-sectional distortions. The theory of reference 1 includes the effects of transverse shear, shear lag, and longitudinal inertia; whereas, the theory of reference 2 includes the effect of restraint of warping and longitudinal inertia. In the calculations presented herein, longitudinal inertia terms were neglected.

For convenience, the frequency equations used in the calculations are presented in the appendix along with the numerical values of the parameters for each beam. The calculated frequencies for the first six bending and the first six torsion modes of beams 1 and 2, along with the experimental frequencies, are presented in tables 1 and 2, respectively.

DISCUSSION OF RESULTS

Since overall dimensions of the two beams were very nearly the same, and since mass distribution and moment of inertia are proportional to cover-sheet thickness, elementary theory predicts almost identical frequencies for corresponding modes. In the lower modes, these beams behave primarily as simple beams, as shown by a comparison of the experimental frequencies in tables 1 and 2. For the higher modes, however, corresponding natural frequencies are lower for the beam with thinner cover sheets (beam 1). The difference between frequencies of corresponding modes of the two beams becomes progressively greater as the mode number increases.

Comparisons of the nodal patterns in figures 5 and 6 show that for practically any given mode the effects of panel vibrations are greater for the beam with the thinner cover sheet (beam 1). Also, the extra or panel modes shown in figures 7 and 8 start at lower frequencies for beam 1 than for beam 2. It may be noted that 12 or more beam modes are present below the frequency of the lowest extra mode for each beam. Thus, decreasing cover-sheet thickness of monocoque beams, all other dimensions being held constant, decreases natural beam frequencies by increasing the susceptibility of the beam modes to secondary effects.

Further evidence of the effects of varying cover-sheet thickness can be gained from the following observations of the information contained in tables 1 and 2. For bending, the differences between calculated frequencies in columns (3) and (4) of tables 1(a) and 2(a) are due to transverse shear and shear lag, whereas the differences between the frequencies given in columns (2) and (4) are believed to be due largely to the effects of panel vibrations. Similar trends have been pointed out for a monocoque beam of rectangular cross section in reference 4. For the beam with thicker cover sheets, the differences between frequencies given by elementary theory and experiment are accounted for by the effects of transverse shear and shear lag. However, for the beam with thinner cover sheets, the differences between frequencies given by elementary theory and experiment are seen to include the effects of panel vibrations in addition to the effects of transverse shear and shear lag. For example, the theory of reference 1

predicts frequencies within 12 percent of experiment for only the first three bending modes of beam 1, whereas for beam 2 comparable accuracies were obtained for the first six bending modes. These results indicate that the frequencies of monocoque beams with thin cover sheets cannot be satisfactorily predicted by beam theory that includes the effects of transverse shear and shear lag but neglects the coupling between panel modes and beam modes.

The calculated torsional frequencies presented in tables 1(b) and 2(b) were obtained from theories which assume that the shape of the beam cross section is maintained and, thus, neglect the effects of coupling between beam modes and panel modes. Hence, the agreement between calculated and experimental torsional frequencies was expected to be unsatisfactory for monocoque beams. Also, the differences between frequencies calculated from elementary theory and those calculated from theory which includes the effect of restraint of warping were expected to be small since the shape of the beam cross section approximated that of a shallow diamond cross section, which has no restraint of warping. Both the theory of reference 2 and elementary theory give calculated frequencies within 12 percent of experiment for the first two torsion modes of beam 2. For beam 1 neither theory predicts values for the lowest torsion frequency within 12 percent of experiment. A comparison of the results in tables 1(b) and 2(b) shows that the effect of decreasing the cover-sheet thickness of a monocoque beam, all other dimensions being held constant, is to reduce the natural torsional frequency.

CONCLUDING REMARKS

Vibration tests were conducted on two 4-percent-thick circular-arc monocoque beams which differed only in thickness of the cover sheet. In addition, natural frequencies were calculated from theories based on rigid cross sections. For the beam with thicker cover sheets, accuracies within 12 percent of experiment were obtained for the first six bending modes and the first two torsion modes. For the other beam, comparable accuracies were obtained for only the first three bending modes. Several extra modes not predicted by the theories were obtained for each beam in the frequency ranges of the tests. These extra modes were associated with panel vibrations and cross-sectional distortions.

Langley Research Center,
National Aeronautics and Space Administration,
Langley Field, Va., June 1, 1959.

APPENDIX

CALCULATIONS FOR BEAM VIBRATION MODES

In this appendix the equations presented and the symbols used are essentially the same as in reference 1 for beam bending modes and in reference 2 for beam torsion modes. Therefore, the reader is cautioned to observe that the definitions for the symbols are not interchangeable. For this reason, most of the symbols are defined separately for the bending modes and the torsion modes. The following symbols, however, are the same throughout the appendix:

b	half-width of beam measured from median line, 17.5 in.
E	modulus of elasticity, 10.6×10^6 lb/sq in.
G	shear modulus of elasticity, 4.0×10^6 lb/sq in.
L	half-length of beam, 70 in.
n,i	integers
R	design radius of curvature of cover sheets, 250 in.
s	distance along perimeter of cross section, in.
ω	natural circular frequency, radians/sec
ρ	distance from centroid of cross section to tangent to median line of cover sheet, $R - (R - h)\cos\frac{s}{R}$, in.
h	maximum vertical distance from centroid of cross section to median line of cover sheet, in. (for beam 1, 0.72 in.; for beam 2, 0.65 in.)

The dimensions and coordinate system of the cross section are shown in figure 9.

Beam Bending Modes

The frequency equations for symmetrical and antisymmetrical free-free beam bending modes are given by equations (41) and (52), respectively, in reference 1 and are repeated here for the case in which longitudinal inertia is neglected.

For the symmetrical modes,

$$k_B^2\left[1 + k_B^2 \sum_{n=1,3,5,\ldots}^{\infty} \left(\frac{2}{n\pi}\right)^2 \frac{1}{N_n}\right] = 0 \qquad \text{(A1)}$$

and for the antisymmetrical modes,

$$k_B^2\left[\frac{1}{3} + k_B^2 \sum_{n=2,4,6,\ldots}^{\infty} \left(\frac{2}{n\pi}\right)^2 \frac{1}{N_n}\right] = 0 \qquad \text{(A2)}$$

where

$$N_n = \frac{n^4\pi^4}{32} - \frac{n^6\pi^2 A k_S^2}{16 A_S} \sum_{i=1,2,3,\ldots}^{\infty} \frac{A_i^2}{K^2 i^2\left(k_S^2 n^2 + K^2 i^2\right)} - \frac{1}{2} k_B^2 \qquad \text{(A3)}$$

The definitions of the various parameters, along with their numerical values for each beam, are as follows:

		Beam 1	Beam 2
μ	mass of beam per unit length, lb-sec^2/in.^{2}	0.382×10^{-2}	0.740×10^{-2}
A	cross-sectional area, sq in.	13.08	27.16
t	actual wall thickness, in.	0.187	0.388
I	minimum moment of inertia of cross section, in.^{4}	3.61	6.40
k_B	frequency coefficient, $\omega\sqrt{\frac{\mu L^4}{EI}}$	$4.897\omega \times 10^{-2}$	$5.118\omega \times 10^{-2}$
k_S	coefficient of shear rigidity, $\sqrt{\frac{EI}{A_S G L^2}}$	0.3019	0.2793
K	geometrical parameter, $\sqrt{\frac{16I}{A_S p^2}}$	0.7407	0.6864
p	perimeter of cross section, in.	70.1	70.0
A_S	effective shear-carrying area, $\oint t \sin^2\theta \, ds \approx \frac{p^3 t}{48R^2}$, sq in.	0.0214	0.0444
A_n	Fourier coefficient, $\frac{2}{p}\oint \sin\theta \sin\frac{2n\pi s}{p} ds$	$(0.05674)\left(\sin\frac{n\pi}{2} + \frac{n\pi}{2}\cos\frac{n\pi}{2}\right)$	$(0.05682)\left(\sin\frac{n\pi}{2} + \frac{n\pi}{2}\cos\frac{n\pi}{2}\right)$
θ	inclination of normal to beam surface with vertical axis		

The natural bending frequencies were calculated from equations (A1) and (A2) by trial, by using the numerical values given for the parameters.

Beam Torsion Modes

If the effects of longitudinal inertia are neglected, the frequency equations for the free-free beam torsion modes (eqs. (40) and (51), respectively, of ref. 2) are, for the symmetrical modes,

$$k_T^2\left[1 + k_T^2 \sum_{m=1,3,5,\ldots}^{\infty} \left(\frac{2}{m\pi}\right)^2 \frac{1}{N_m}\right] = 0 \qquad (A4)$$

and for the antisymmetrical modes,

$$k_T^2\left[\frac{pt_a\mu}{2I_p}\left(\frac{2p}{\pi L}\right)^2 \sum_{n=2,4,6,\ldots}^{\infty} \frac{K_n^2}{16n^2} + \left(\frac{2}{\pi}\right)^2 k_T^2 \sum_{n=2,4,6,\ldots}^{\infty} \frac{1}{n^2 N_n} + \frac{1}{3}\right] = 1 \qquad (A5)$$

where

$$N_n = \frac{n^2\pi^2}{8}\left(1 + \frac{pt_aK^2n^2}{2J} \sum_{i=2,4,6,\ldots}^{\infty} \frac{K_i^2}{K^2n^2 + 16i^2}\right) - \frac{1}{2}k_T^2 \qquad (A6)$$

The definitions and numerical values of the parameters in equations (A4), (A5), and (A6) are as follows:

		Beam 1	Beam 2
μ	mass density of beam, lb-sec^2/in.^{4}	0.259×10^{-3}	0.259×10^{-3}
A_o	cross-sectional area enclosed by median line of wall thickness, sq in.	33.6	30.3
I_p	mass polar moment of inertia per unit length, lb-sec^2	0.430	0.789
J	torsional stiffness constant, $\frac{4A_o^2t}{p}$, in.^{4}	12.02	20.40
K	parameter, $\frac{p}{L}\sqrt{\frac{E}{G}}$	1.630	1.628
m	integer		
t_a	actual wall thickness, in.	0.187	0.388
p	perimeter of cross section, in.	70.1	70.0
K_n	Fourier coefficient, $\frac{2}{p}\oint \rho \cos\frac{2i\pi s}{p}\,ds$	$\frac{(-1)^{\frac{i}{2}+1}\ 0.991}{0.00199 - i^2}$	$\frac{(-1)^{\frac{i}{2}+1}\ 0.990}{0.00199 - i^2}$
		$(i = 2,4,6,\ldots)$	
k_T	frequency parameter, $\omega\sqrt{\frac{I_pL^2}{GJ}}$	$0.663\omega \times 10^{-2}$	$0.689\omega \times 10^{-2}$

The roots of the frequency equations (A4) and (A5) were obtained by trial.

REFERENCES

1. Budiansky, Bernard, and Kruszewski, Edwin T.: Transverse Vibrations of Hollow Thin-Walled Cylindrical Beams. NACA Rep. 1129, 1953. (Supersedes NACA TN 2682.)

2. Kruszewski, Edwin T., and Kordes, Eldon E.: Torsional Vibrations of Hollow Thin-Walled Cylindrical Beams. NACA TN 3206, 1954.

3. Kordes, Eldon E., and Kruszewski, Edwin T.: Experimental Investigation of the Vibrations of a Built-Up Rectangular Box Beam. NACA TN 3618, 1956.

4. Kordes, Eldon E., and Kruszewski, Edwin T.: Investigation of the Vibrations of a Hollow Thin-Walled Rectangular Beam. NACA TN 3463, 1955.

TABLE 1.- NATURAL FREQUENCIES OF BEAM 1

(a) Bending frequencies

Mode ①	Experimental frequency, cps ②	Calculated frequency, cps	
		Elementary theory ③	Theory of ref. 1 ④
1	16.95	17.84	17.01
2	40.05	49.20	40.95
3	63.36	96.30	71.24
4	83.75	159.5	105.4
5	102.3	237.5	145.7
6	114.7	332.4	188.2

(b) Torsional frequencies

Mode ①	Experimental frequency, cps ②	Calculated frequency, cps	
		Elementary theory ③	Theory of ref. 2 ④
1	32.82	37.73	37.90
2	43.86	75.46	75.50
3	50.52	113.2	113.5
4	57.73	150.9	152.1
5	71.33	188.7	192.6
6	89.10	226.4	229.8

TABLE 2.- NATURAL FREQUENCIES OF BEAM 2

(a) Bending frequencies

Mode ①	Experimental frequency, cps ②	Calculated frequency, cps	
		Elementary theory ③	Theory of ref. 1 ④
1	16.50	17.40	16.09
2	40.10	47.90	37.42
3	66.78	93.90	64.95
4	93.25	155.9	87.79
5	118.9	222.2	115.2
6	144.1	324.0	141.5

(b) Torsional frequencies

Mode ①	Experimental frequency, cps ②	Calculated frequency, cps	
		Elementary theory ③	Theory of ref. 2 ④
1	35.90	36.36	36.38
2	65.03	72.72	72.99
3	85.21	109.1	109.3
4	102.8	145.4	146.5
5	123.6	181.8	185.7
6	149.7	218.2	222.1

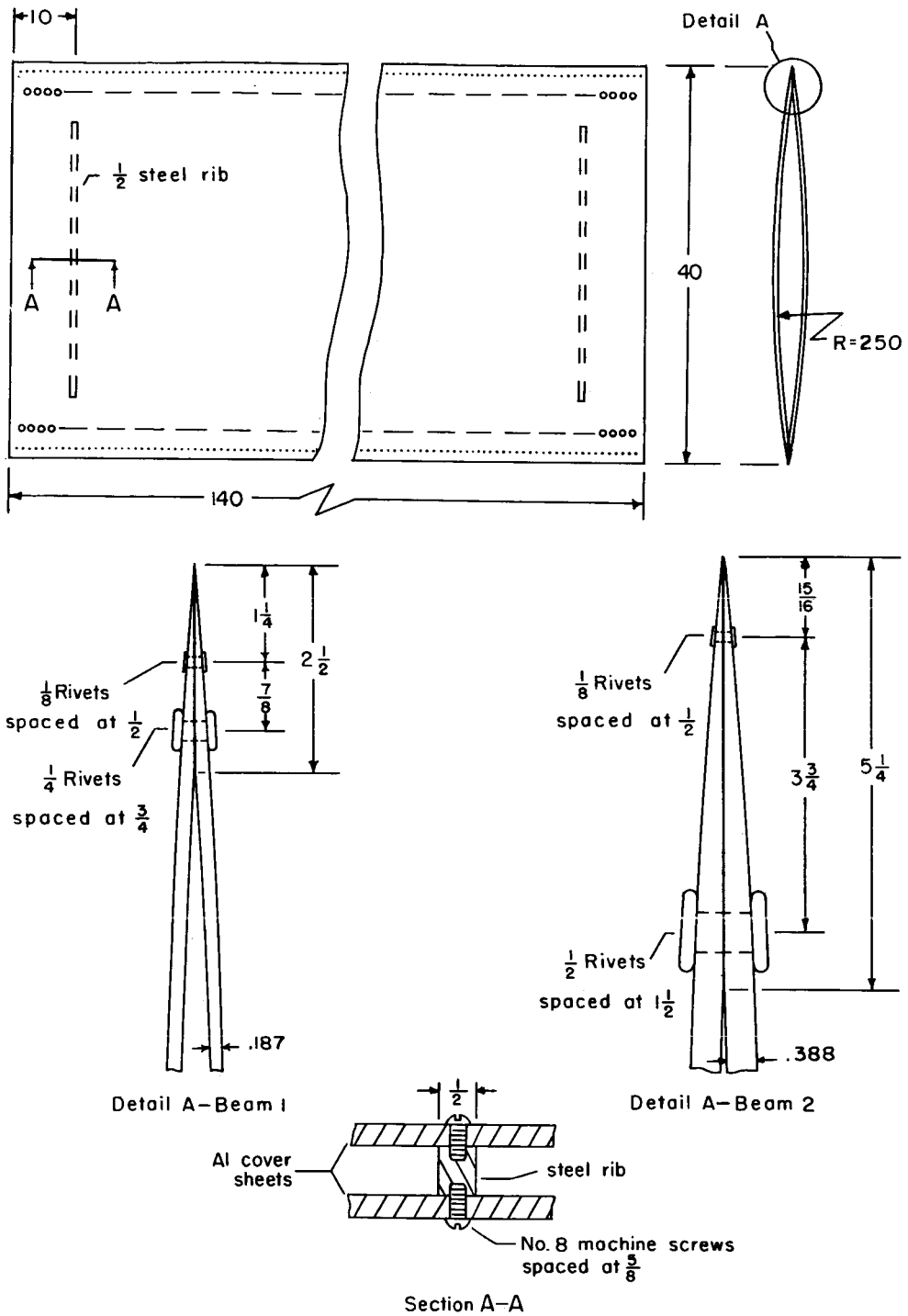

Figure 1.- Plan form and nominal dimensions. All dimensions are in inches.

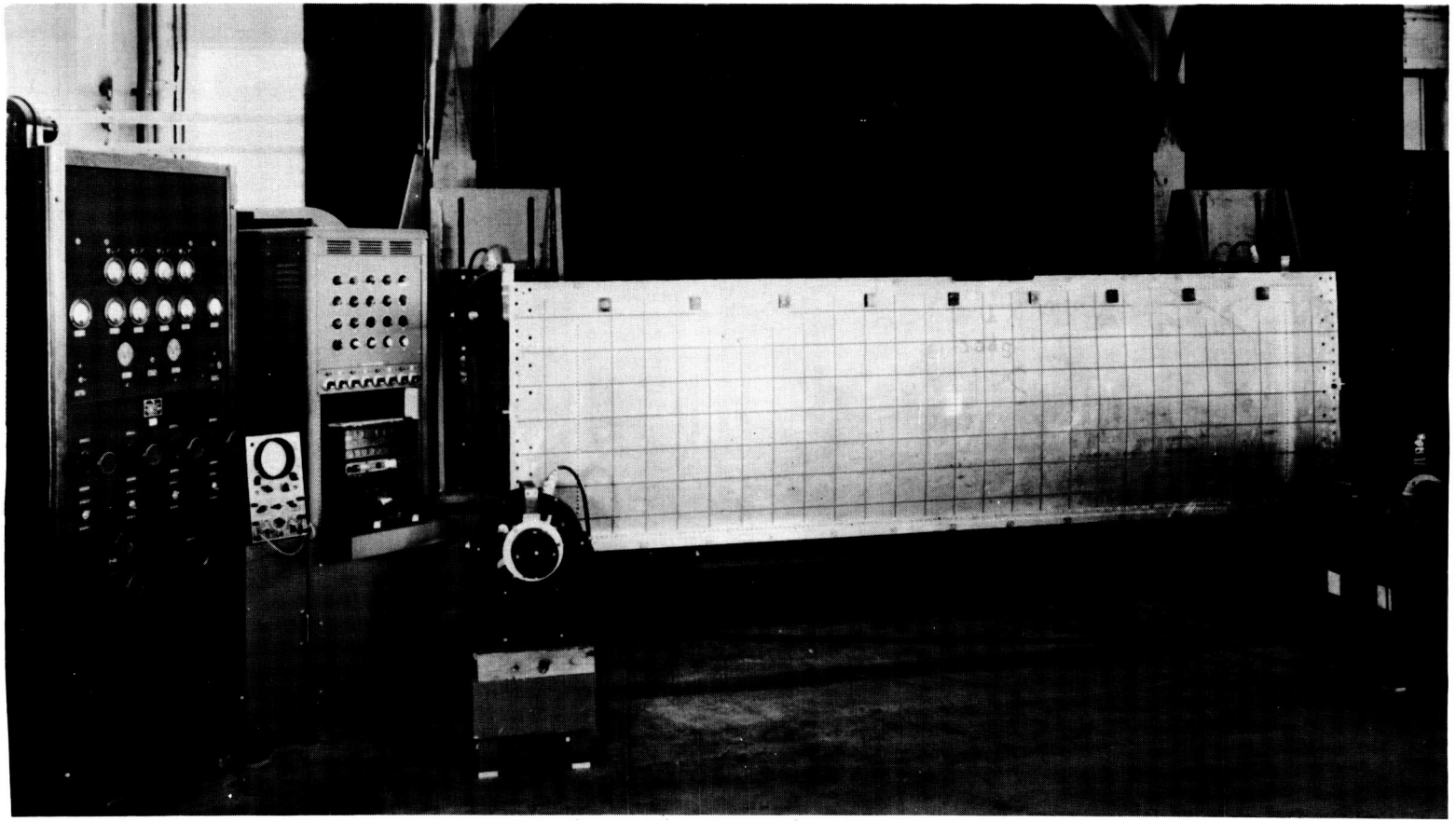

Figure 2.- Test setup. L-58-1347

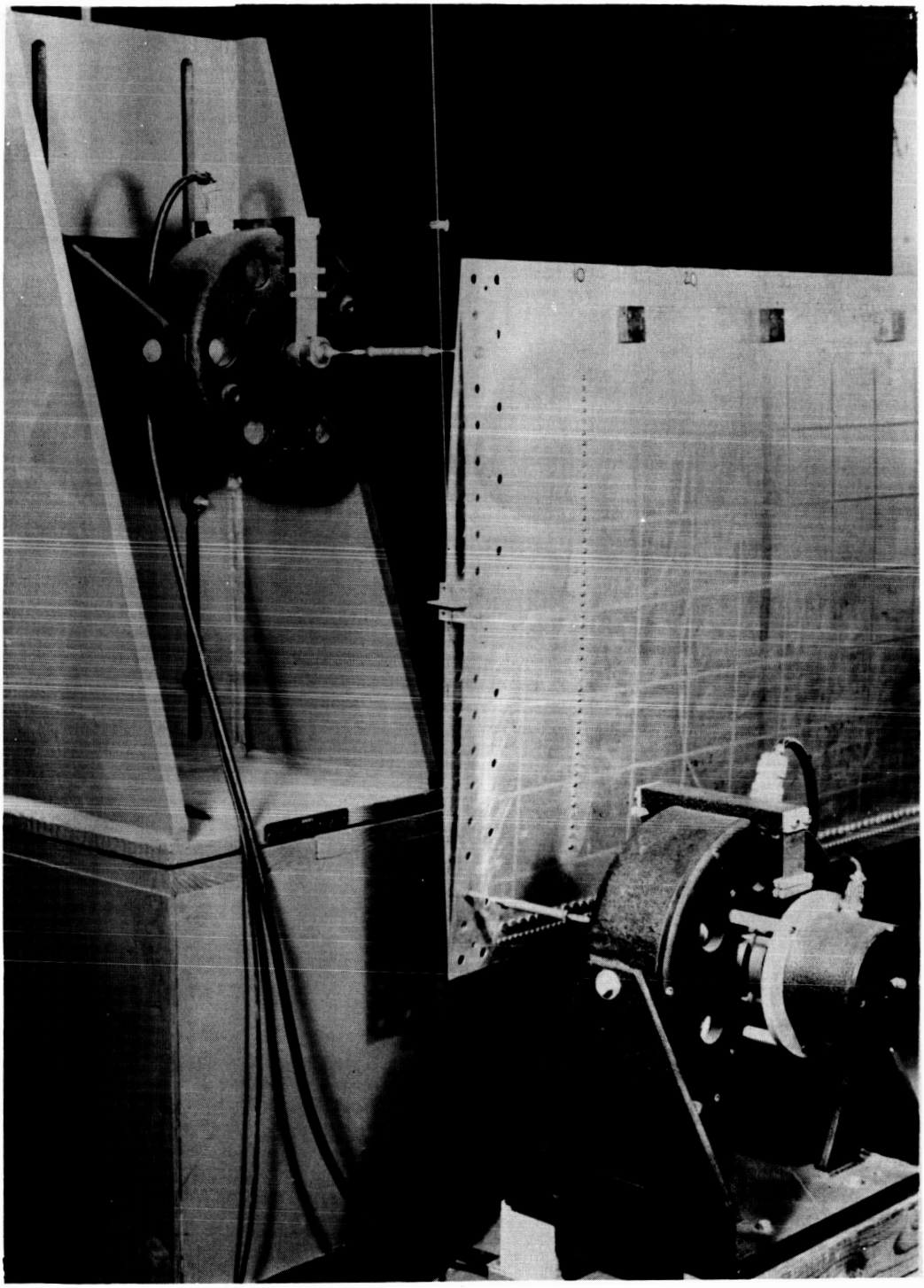

Figure 3.- Shaker attachments and support. L-58-1348

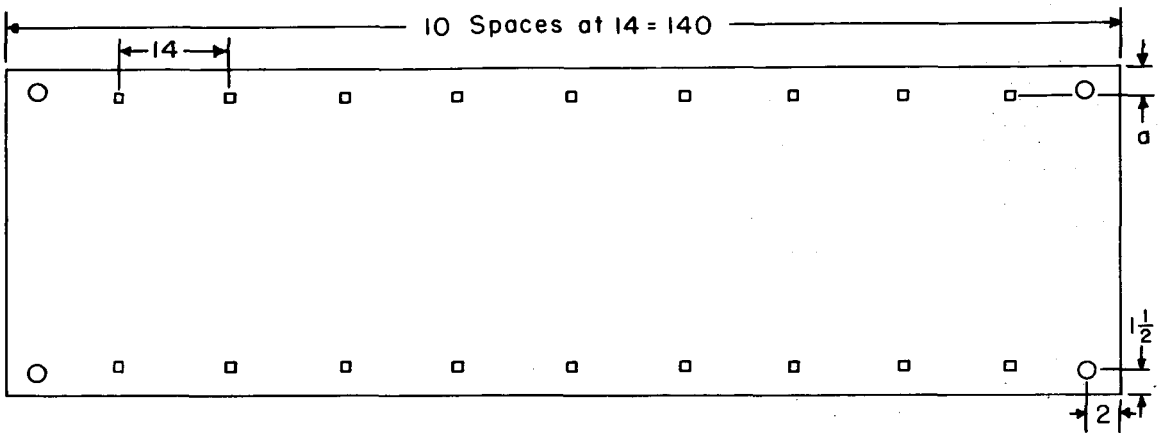

Beam	a
1	$3\frac{5}{16}$
2	$1\frac{5}{16}$

Figure 4.- Locations of shakers, pickups, and counterweights.

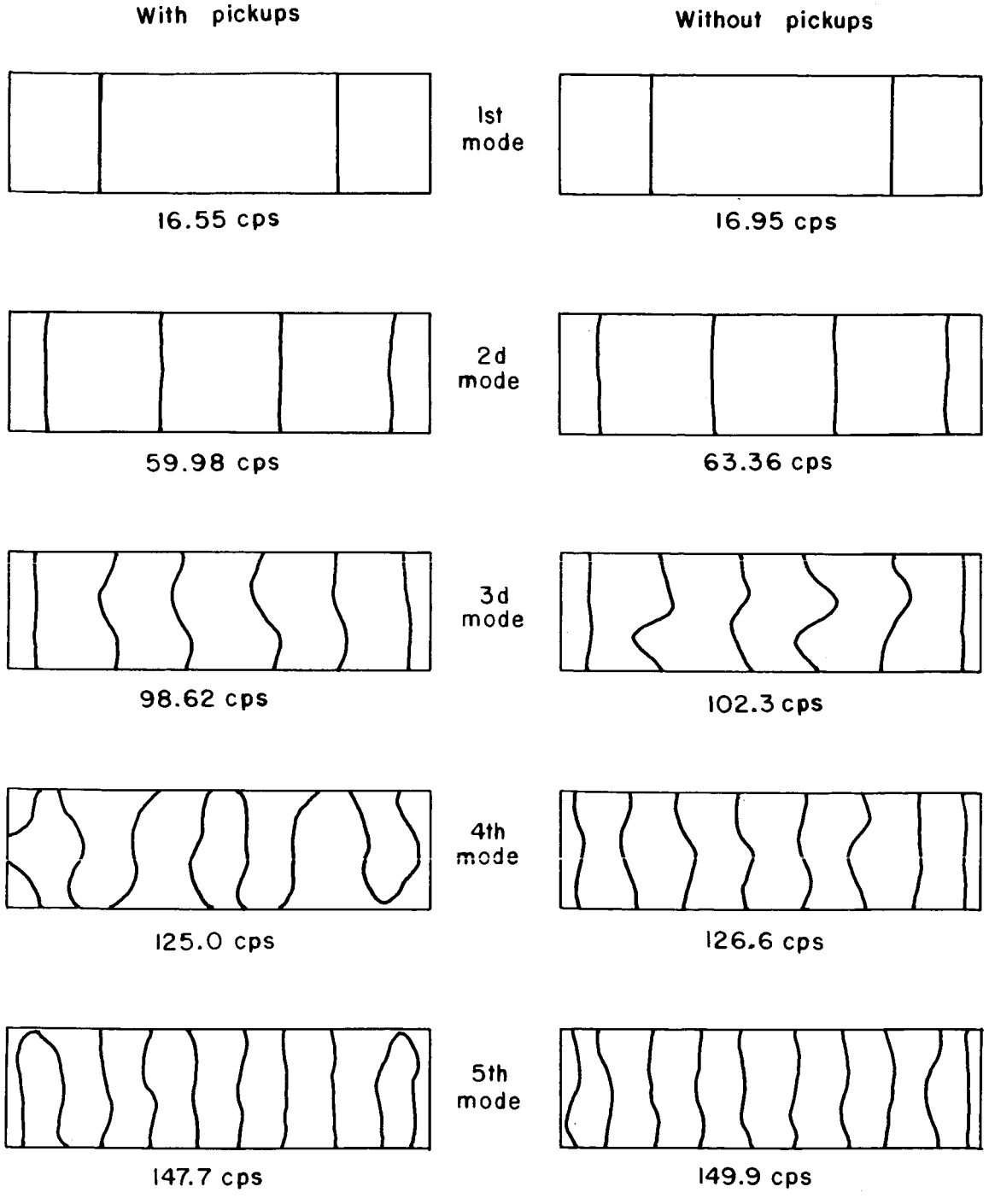

(a) Symmetrical bending modes.

Figure 5.- Beam nodal patterns and frequencies of beam 1.

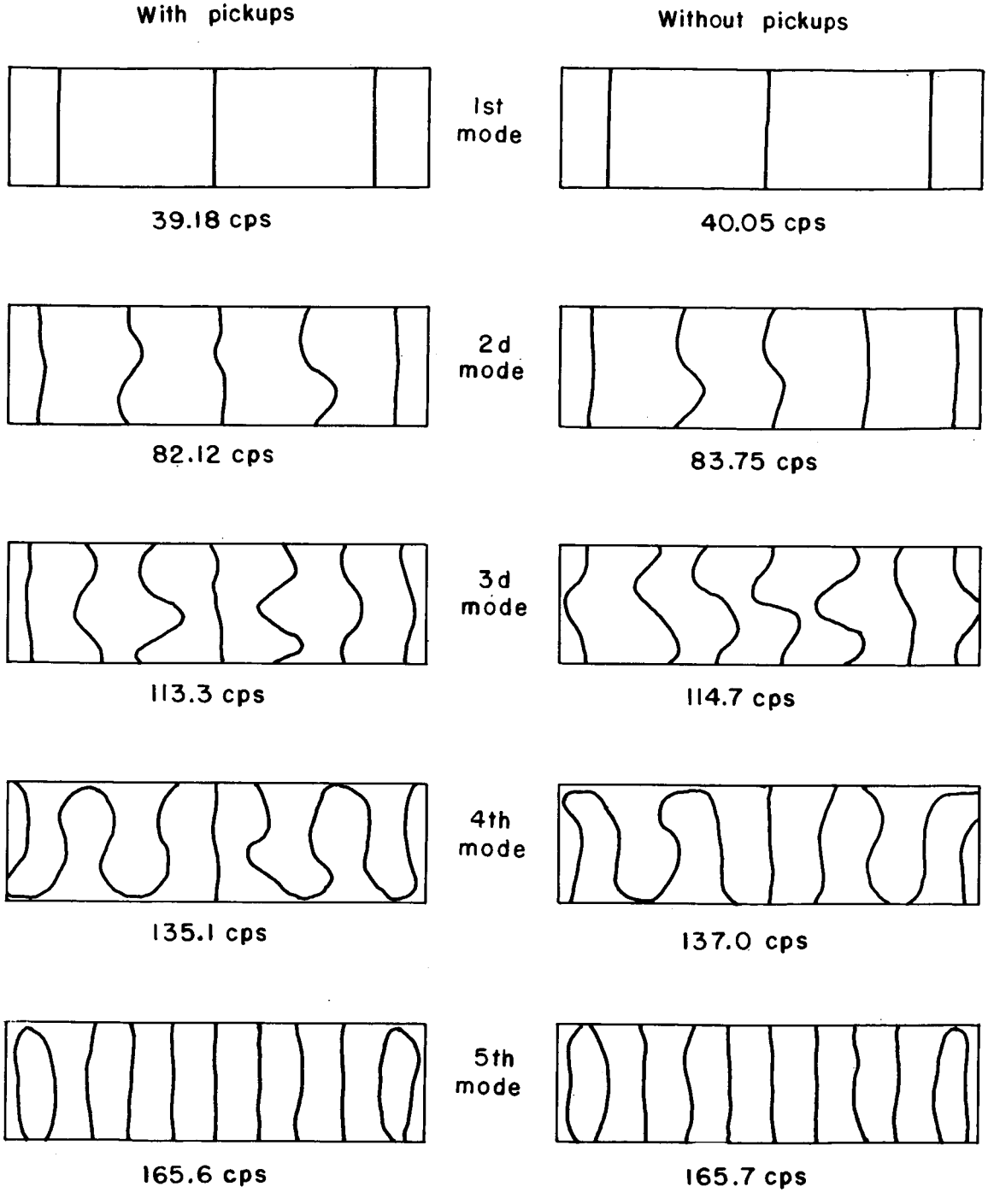

(b) Antisymmetrical bending modes.

Figure 5.- Continued.

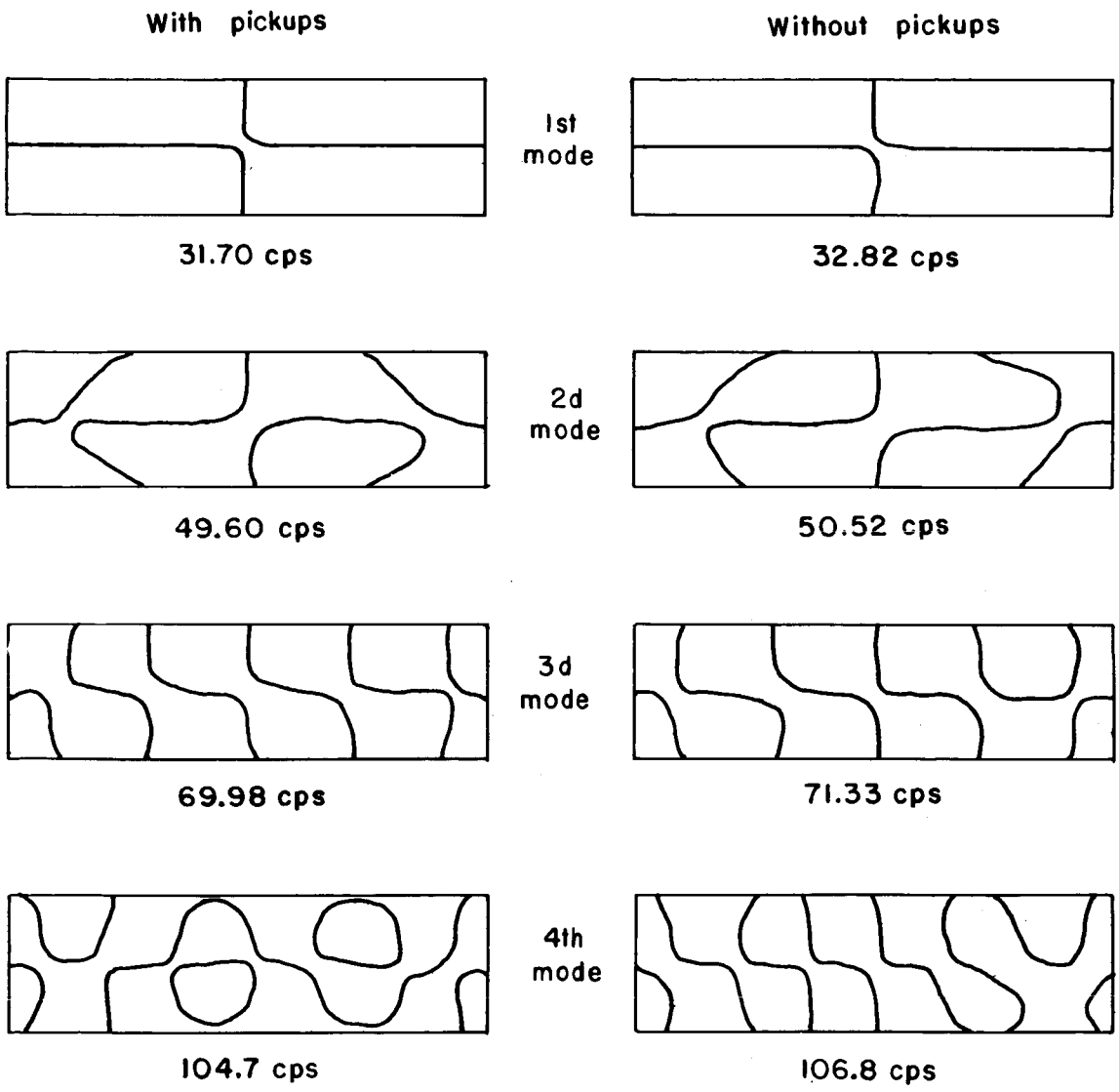

(c) Antisymmetrical torsion modes.

Figure 5.- Continued.

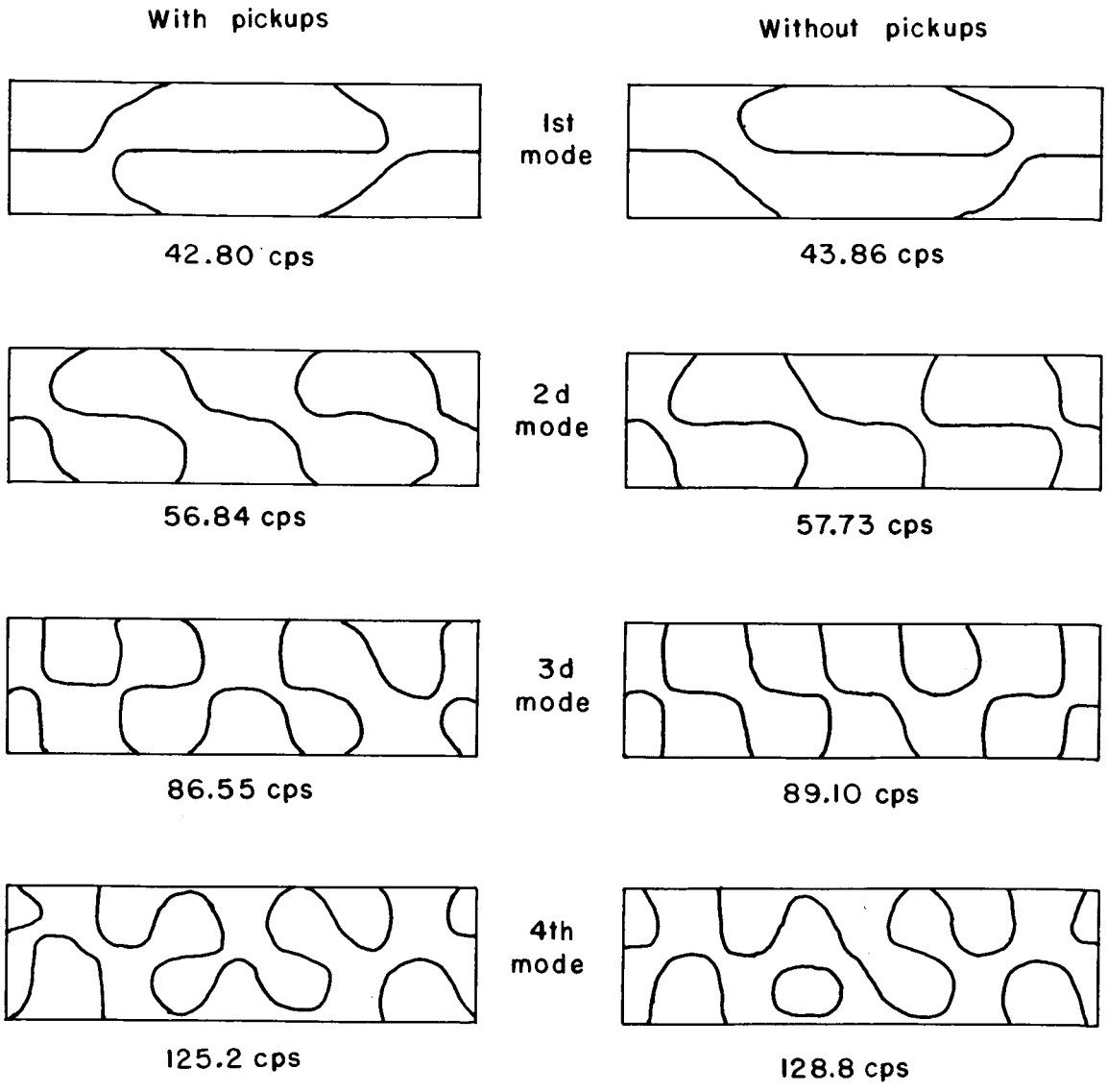

(d) Symmetrical torsion modes.

Figure 5.- Concluded.

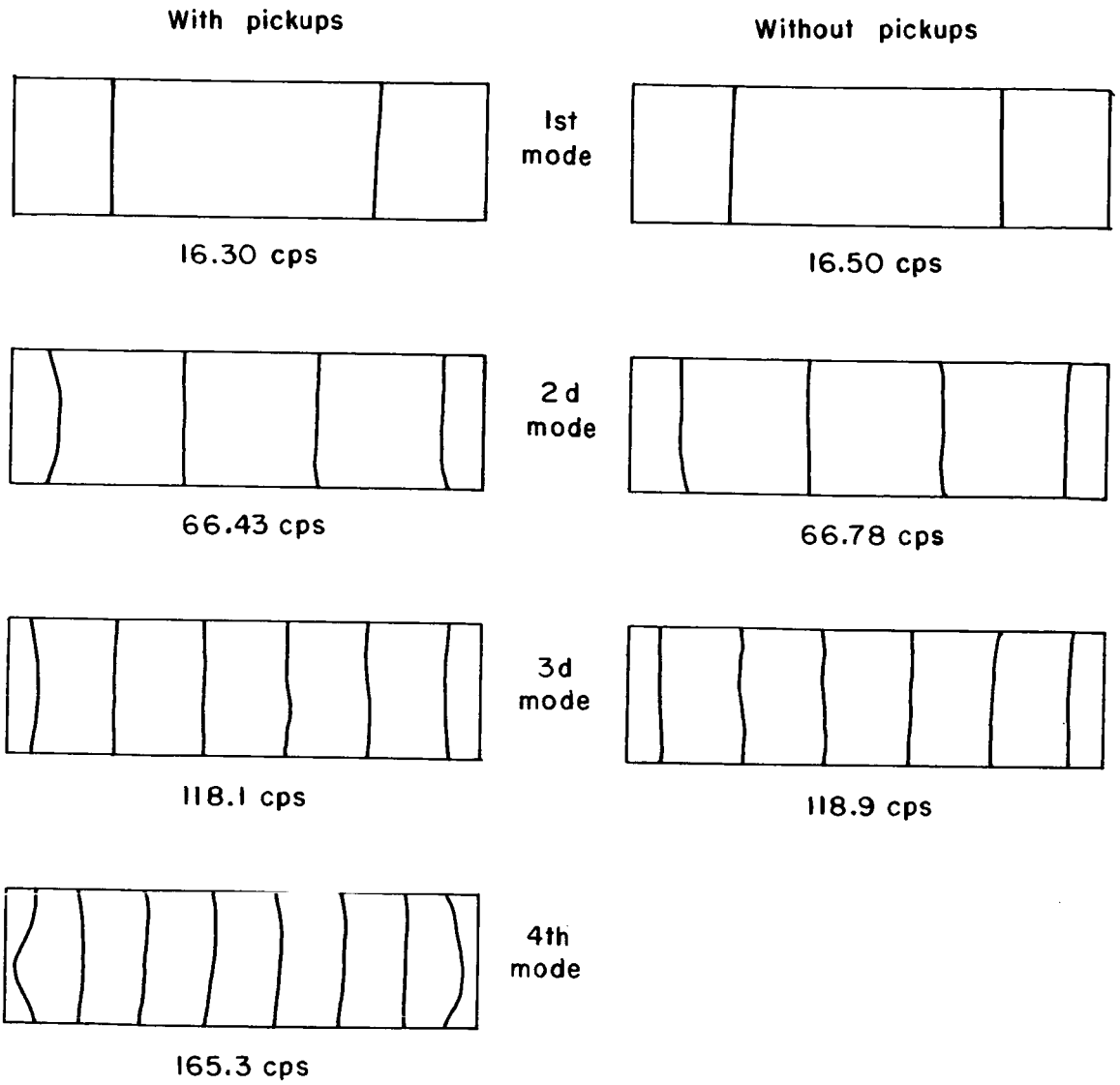

(a) Symmetrical bending modes.

Figure 6.- Beam nodal patterns and frequencies of beam 2.

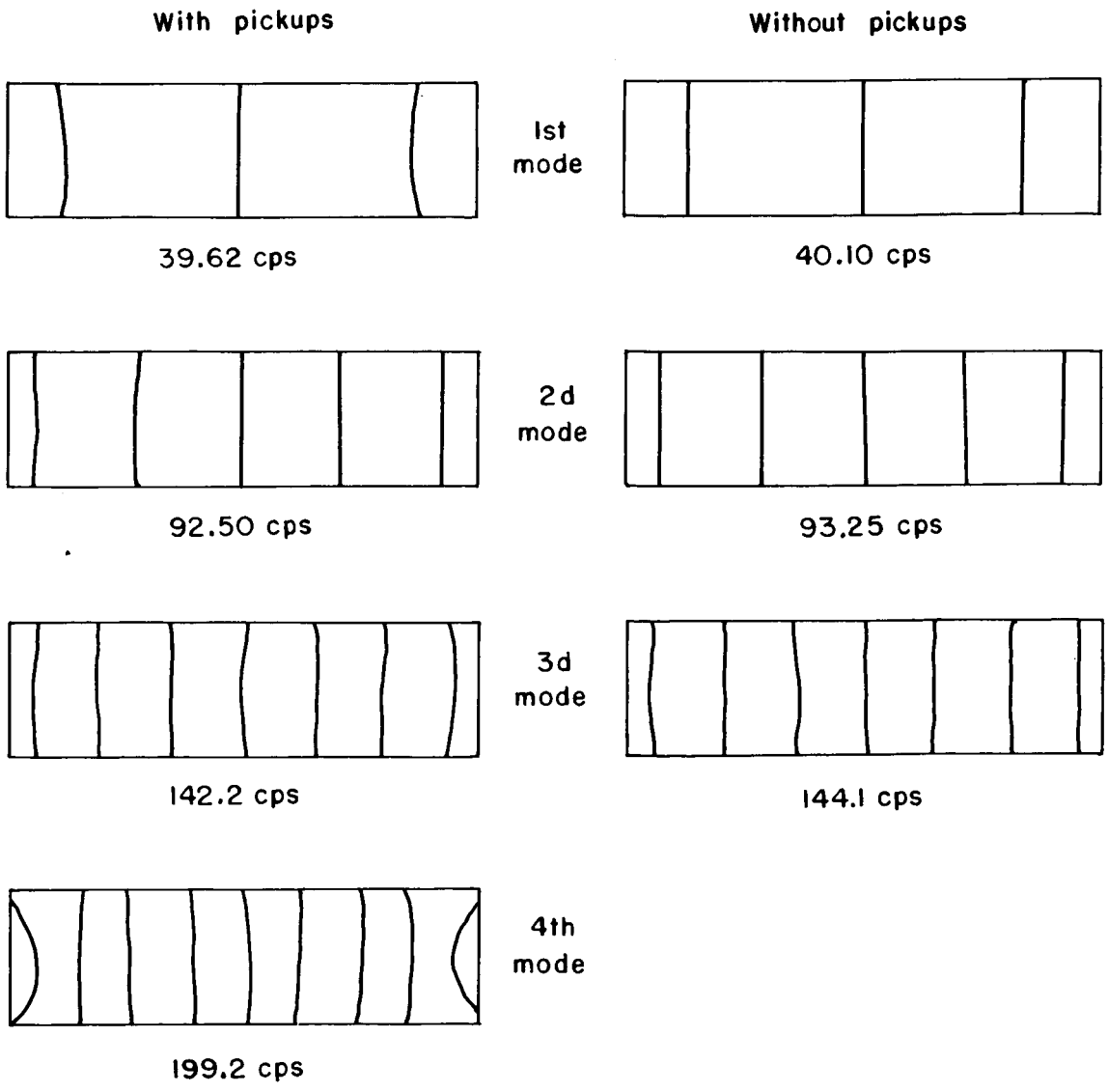

(b) Antisymmetrical bending modes.

Figure 6.- Continued.

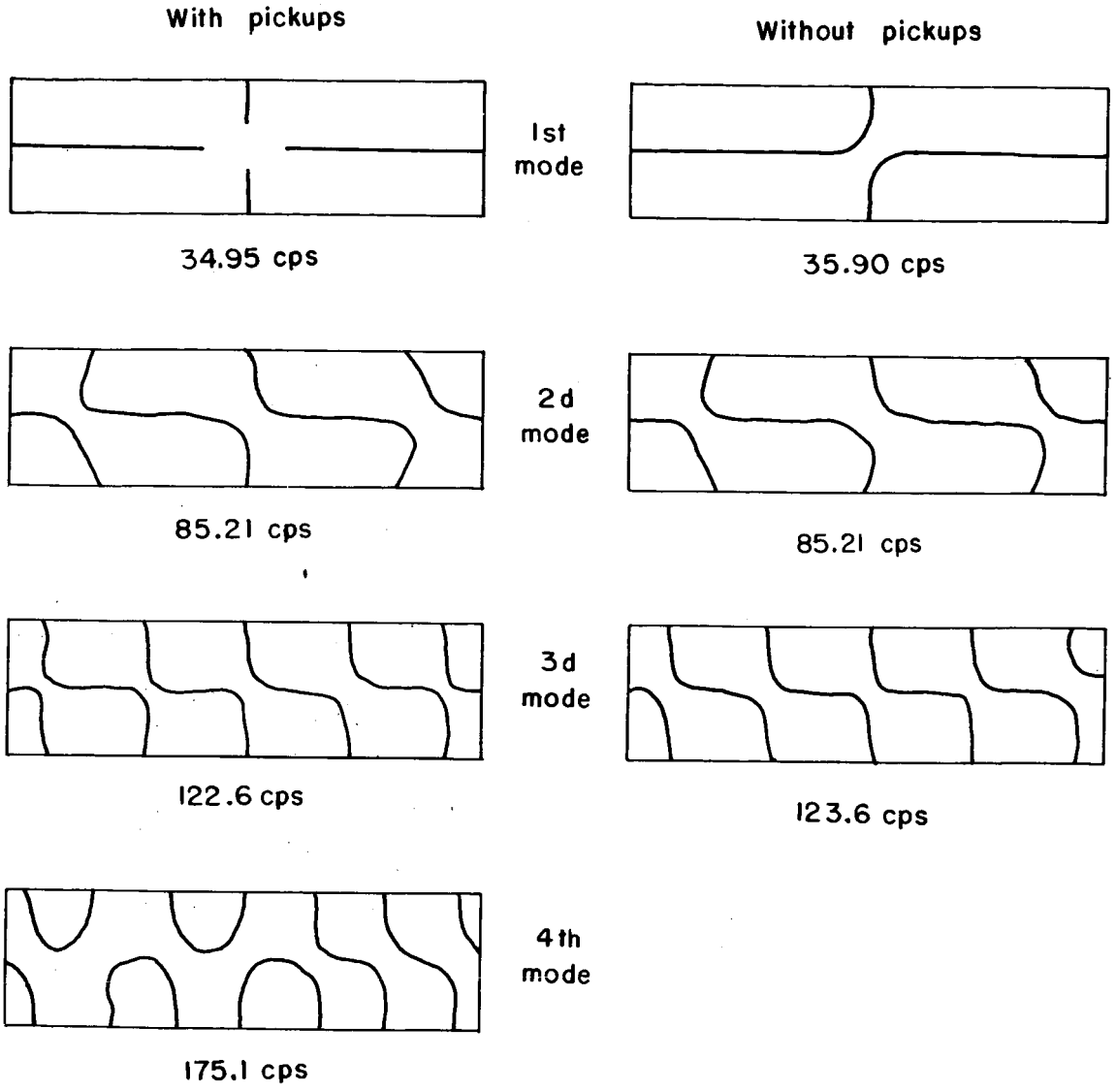

(c) Antisymmetrical torsion modes.

Figure 6.- Continued.

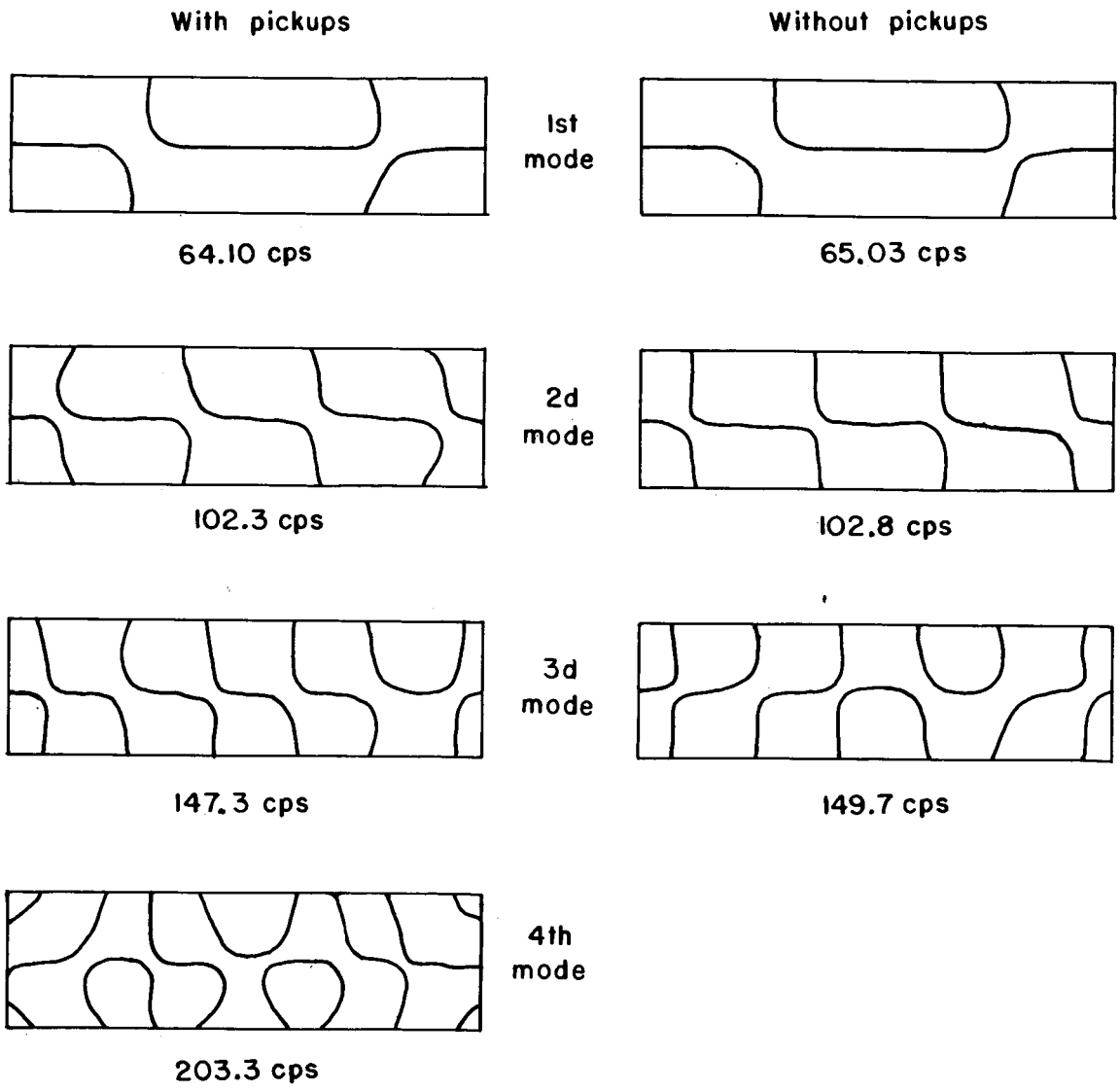

(d) Symmetrical torsion modes.

Figure 6.- Concluded.

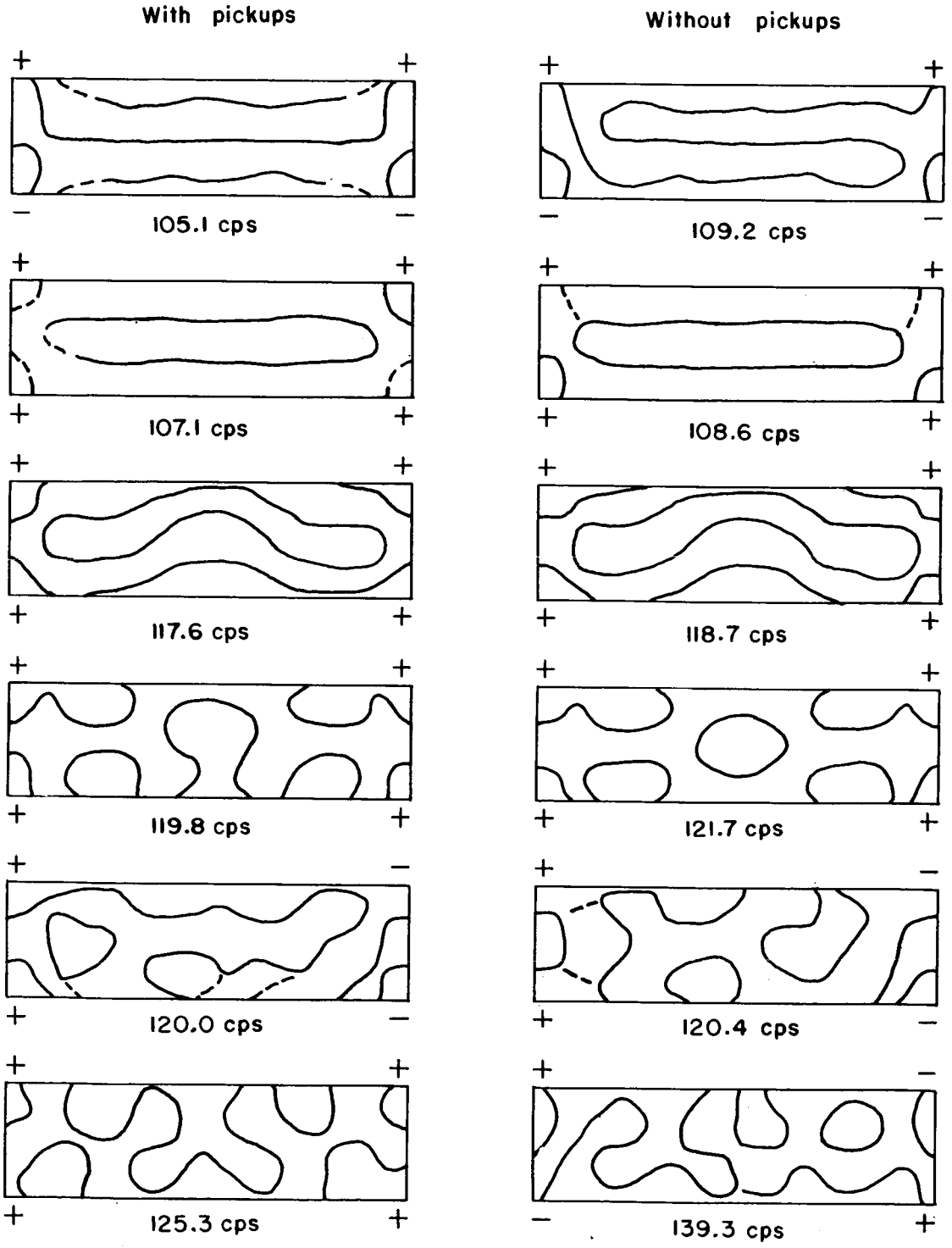

Figure 7.- Nodal patterns and frequencies of panel modes of beam 1.

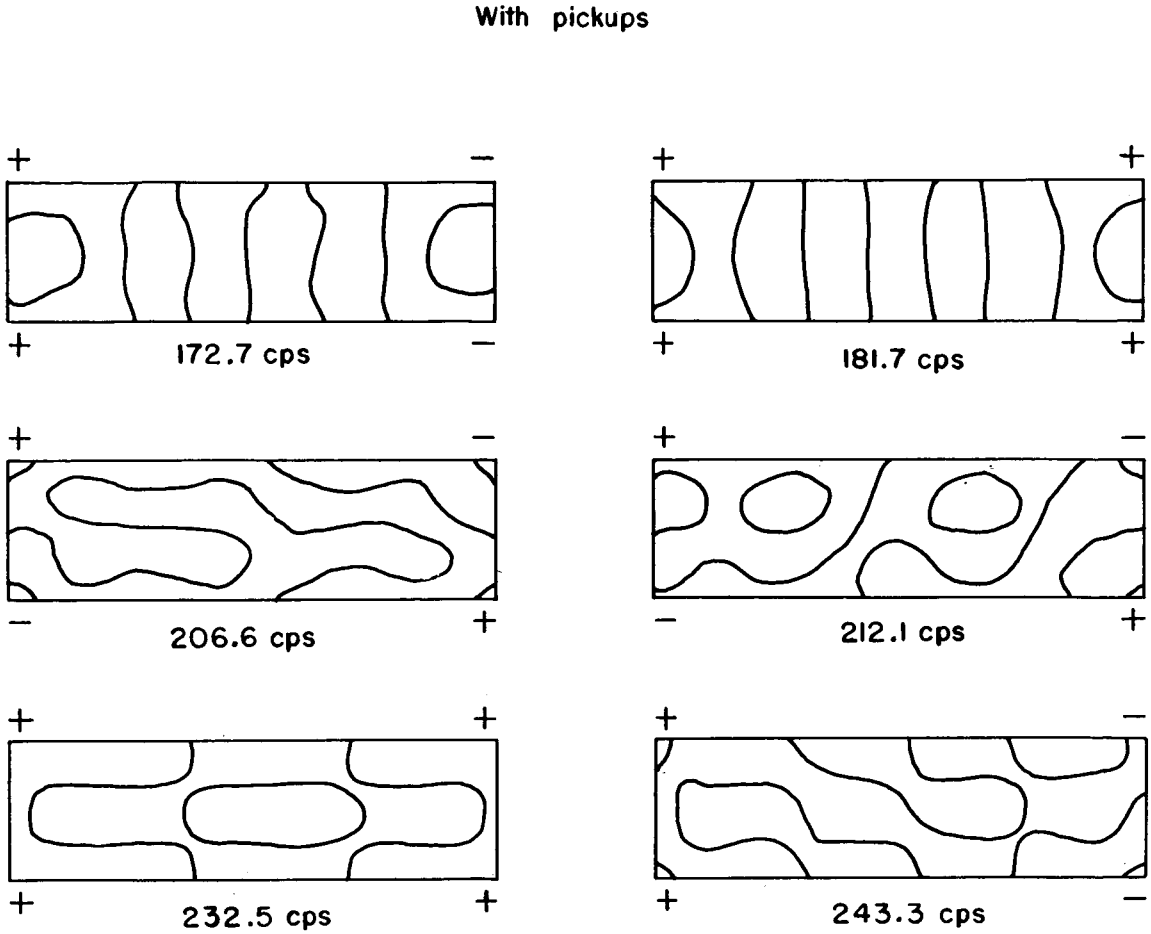

Figure 8.- Nodal patterns and frequencies of panel modes of beam 2.

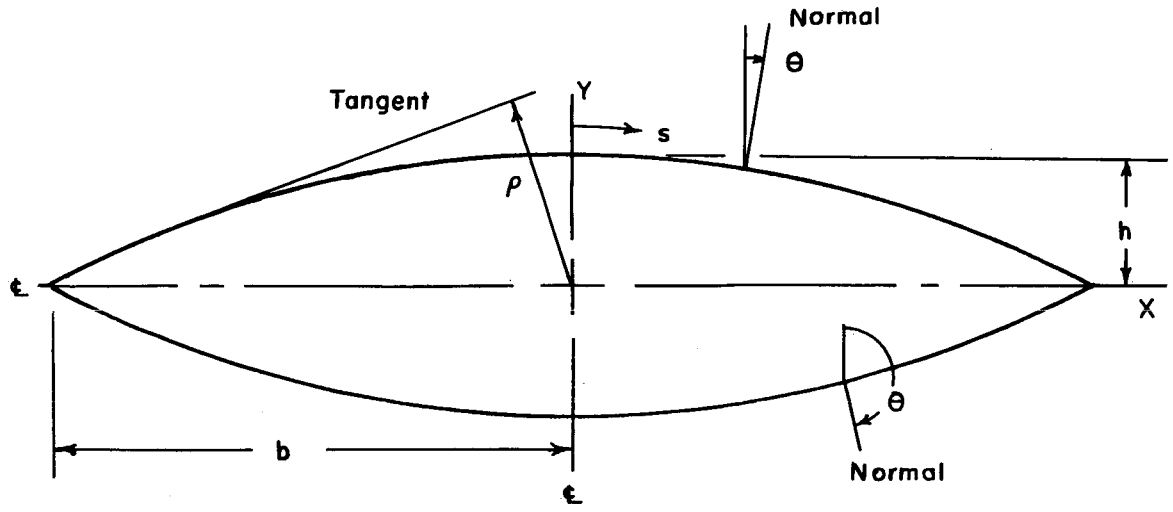

Figure 9.- Coordinate system.